HHS Public Access

Author manuscript

Nat Med. Author manuscript; available in PMC 2014 September 01.

Published in final edited form as:

Nat Med. 2014 March ; 20(3): 265–271. doi:10.1038/nm.3465.

P38 MAPK signaling underlies a cell autonomous loss of stem cell self-renewal in aged skeletal muscle

Jennifer D. Bernet[1], **Jason D. Doles**[1], **John K. Hall**[1,2], **Kathleen Kelly-Tanaka**[1], **Thomas A. Carter**[1], and **Bradley B. Olwin**[1,*]

[1]Molecular, Cellular and Developmental Biology, University of Colorado, Boulder, CO 80309

Abstract

Skeletal muscle aging results in a gradual loss of skeletal muscle mass, skeletal muscle function and decreased regenerative capacity, which can lead to sarcopenia and increased mortality. While the mechanisms underlying sarcopenia remain unclear, the skeletal muscle stem cell, or satellite cell, is required for muscle regeneration. Therefore, identification of signaling pathways affecting satellite cell function during aging may provide insights into therapeutic targets for combating sarcopenia. Here, we show that a cell-autonomous loss in self-renewal occurs via alterations in FGF Receptor 1 and p38αβ MAPK signaling in aged satellite cells. We further demonstrate that pharmacological manipulation of these pathways can ameliorate age-associated self-renewal defects. Thus, our data highlight an age-associated deregulation of a satellite cell homeostatic network and reveal potential therapeutic opportunities for the treatment of progressive muscle wasting.

Introduction

Sarcopenia, defined as an irrevocable loss of skeletal muscle mass and strength in aged individuals[1,2], results in frailty and a high risk of mortality[3,4], thus greatly increasing government healthcare expenditures compunded by an expanding elderly population[5]. The mechanisms involved in the development of sarcopenia are poorly understood but include changes in skeletal muscle metabolism, compromised regeneration and muscle stem cell function[6-9]. Widely regarded as critical to the regeneration process, satellite cells (SCs) reside next to the myofiber plasma membrane of young skeletal muscle myofibers[10]. Indeed, ablation experiments demonstrate that SCs are bona-fide muscle stem cells as they exhibit remarkable regenerative and self-renewing properties[11-13].

*Address correspondence to: Bradley Olwin, Professor, Molecular Cellular and Developmental Biology, 347 UCB, MCD-Biology, Boulder CO 80309, Phone: 303 492-6816, Fax: 303 492-1587, bradley.olwin@colorado.edu.

[2]Current address: Department of Neurology, University of Washington, Seattle, WA 98195-7720

Supplementary Information: Supplementary information is available in the online version of the paper.

Author Contributions: J.D.B. and B.B.O. conceptualized the study. J.D.B. performed and analyzed the experiments. J.K.H. assisted with transplantation experiments. K.K.T. designed and performed the collection of microarray data. J.D.D. performed the microarray analysis. T.A.C. assisted with image scoring. J.D.B, B.B.O and J.D.D. wrote, discussed and edited the manuscript. B.B.O. supervised the project.

Author Information: Microarray CEL files are deposited in NCBI. The authors declare no competing financial interests.

The poor regenerative capacities of sarcopenic muscle are reportedly due to environmental impairment of aged SC function[6,7,9,14-16]. Systemic cues within the aged environment compromise SC activity, and exposure to a young environment improves regeneration of aged muscle and SC differentiation[17-22]. Notably, the effects of the aged environment can be overcome as transplantation of young myofibers with their attached SCs prevents age-associated loss of muscle mass and strength[23].

FGF receptor (FGFR) tyrosine kinases play important roles in coordinating extracellular signals with internal SC regulatory networks. While FGFRs indirectly promote proliferation by repressing myoblast differentiation, they do not directly function as mitogens[24]. SCs express FGF Receptor-1 (FGFR1) and FGF Receptor-4[25,26]where FGF Receptor-4 plays a role in cell fate determination during embryonic muscle development[27] and FGFR1 prevents terminal differentiation[28,29]. Intracellular signals activated by FGFR1 include both ERK and p38αβ MAPK pathways, which regulate SC proliferation and asymmetric division, respectively[30,31].

Members of the MAPK family play diverse and complicated roles in the maintenance, proliferation, asymmetric division and differentiation of SCs. ERK is necessary but not sufficient for myoblast proliferation[30,32] and does not regulate differentiation[28,30], but is implicated in age-related loss of SC proliferative capacity[32]. Signaling by p38αβ MAPK is involved in the exit of SCs from quiescence[31,33], asymmetric division of SCs[33], and differentiation of SCs *in vivo*[33]. The p38αβ MAPKs and p38γ MAPK also play roles in myogenic differentiation[34,35]. Because of the diverse roles that MAPKs play in regulating SC function, their relative activities are likely spatially and temporally context dependent.

Here we show that aged SCs possess a cell-autonomous defect in self-renewal that cannot be rescued by exposure to a young environment. We demonstrate that these cell intrinsic deficits arise from an impaired response to FGF ligands and elevated p38αβ MAPK activity, which when corrected, rescue aged SC self-renewal. Thus, our data identify cell autonomous FGF/p38αβ MAPK signaling as a critical pathway deregulated in aged SCs and highlight a novel therapeutic opportunity for clinical management of age-associated sarcopenia.

Results

A young environment does not rescue an age-associated self-renewal deficit

Myofiber-associated aged SCs fail to expand as efficiently as young SCs (Fig. 1a, Supplementary Fig. 1a–e) and aged SCs are prone to differentiation when compared to young SCs (Fig. 1a)[18,36]. Since parabiosis and transplantation experiments show that a young environment restores aged SC function[18,21,22], we developed a heterochronic culture assay (Fig. 1b) to specifically assess whether a young local environment (intact myofibers) could restore aged SC expansion. SCs isolated from young or aged mice constitutively expressing GFP (*βActGFP*) were seeded onto unlabeled myofibers from a young mouse and fixed for analysis at 24 h (Fig. 1c) and 72 h after seeding (Fig. 1d). Quantification of endogenous host SCs marked by Syndecan-4[37] (*, Fig. 1c) and donor GFP$^+$ SCs (Fig. 1c,d) revealed equivalent young and aged donor SC attachment at 24 h (Fig. 1e). We observed 3-

fold more young donor cells present at 72 h in culture compared to aged donor cells (Fig. 1f).

Seeding of aged SCs onto young myofibers failed to rescue aged SC expansion and thus, we hypothesized that a young global environment, including circulating factors, may be necessary to rescue aged SC self-renewal and subsequent expansion. Therefore, we transplanted young and aged *βActGFP* myofiber-associated SCs into young wild-type hosts concurrent with $BaCl_2$ injury[23] (Fig. 1g, Supplementary Fig. 1f–g). Although young and aged SCs fused into host myofibers (Fig. 1h), we detected a 50% reduction in aged donor-derived cells in the SC position 30 d post-transplantation compared to young donor-derived SCs (Fig. 1i). By 60 d post-transplantation, we detected few aged donor-derived SCs, whereas young donor-derived cell numbers remained constant (Fig. 1i,j).

Self-renewal and p38 MAPK signaling are impaired in aged SCs

Transplanted, aged SCs were not maintained in a young host environment so we tested whether aged SCs were capable of generating quiescent daughter cells in culture (Fig. 2a–d)[33]. Myofibers treated with the mitotoxin 1β-arabinofuranosylcytosine (AraC) for 3–5 d post-isolation yielded similar numbers of surviving SC daughters in young and aged cultures but a lower number of quiescent $Pax7^+$ daughters and a greater number of post-mitotic, differentiated cells in aged cultures compared to young cultures (Fig. 2b,d). AraC was then washed out and cultures were maintained for an additional 3 d to assess myoblast expansion and SC self-renewal as previously described[33]. In contrast to young cultures, aged myofiber-associated SCs were incapable of further expansion and self-renewal upon AraC removal (Fig. 2c, d).

One explanation for the poor engraftment of aged SCs is that the cells fail to properly activate. Given the prominent role of p38αβ MAPK signaling in regulating SC activation[31] and asymmetric division[33], we systematically interrogated the integrity of this signal transduction cascade in aged SCs. Young myofiber-associated SCs activate within 30 min of injury or explantation as measured by p38αβ MAPK phosphorylation[31]. Surprisingly, we found enhanced p38αβ MAPK phosphorylation (phospho-p38) in aged myofiber-associated SCs compared to young SCs analyzed 1 h post-isolation (Fig. 2e,f) as well as increased phosphorylated MAPKAPK2 (pMK2), a direct target of p38αβ MAPK (Fig. 2e,f). Consistent with these culture data we observed a 4-fold increase of pMK2 in sublaminar SCs in aged compared to young skeletal muscle sections (Fig 2g,h).

To investigate the molecular mechanisms underlying aged SC behavior, we collected RNA from FACS-isolated SCs pooled from multiple animals for an unbiased gene expression analysis to identify gene ontology (GO) terms and molecular pathways that change significantly between young and aged SCs. We identified a general reduction of gene expression associated with asymmetric division[33] (Fig. 3a, Supplementary Fig. 2), cell growth and differentiation in aged compared to young SCs (Supplementary Fig. 3, Supplementary Table 1). Since SCs are capable of self-renewal driven by asymmetric activation of p38αβ MAPK[33], we expected a reduction in aged SC asymmetric phospho-p38, despite their elevated p38 signaling. Quantitative analysis of myofiber-associated SCs (Fig. 3b, Supplementary Video 1) revealed a 50% reduction in asymmetric phospho-p38

compared to young SCs (Fig. 3c). Inhibition of p38αβ MAPK signaling with 25 μM SB203580 virtually eliminated asymmetric phospho-p38$^+$ young and phospho-p38$^+$ aged SCs (Fig. 3c, Supplementary Fig. 4). Notably, partial inhibition of p38αβ MAPK signaling enhanced asymmetric phospho-p38 in aged SCs but not young SCs (Fig. 3c).

The restoration of asymmetric phospho-p38 by partial inhibition of p38αβ MAPK suggests that self-renewal in aged SCs may be similarly rescued. We assayed aged SC self-renewal using a previously published dye retention assay[33] whereby cell permeable carboxyfluorescein diacetate-succinimidyl ester (CFDA-SE) is acquired by all cells but is retained only in quiescent or differentiated non-cycling cells (Fig. 3d,e). Quiescent Pax7$^+$ SCs that retained CFDA-SE were present in young but dramatically reduced in aged cultures (Fig. 3f). Partial inhibition of p38αβ MAPK with either SB203580 or BIRB 796 (Fig. 3f, Supplementary Fig. 4) restored the aged label-retaining, Pax7$^+$ SC numbers to near young levels (Fig. 3f).

A spatiotemporal FGF-p38αβ MAPK pathway is involved in SC self-renewal

Increased FGF-2 in aged skeletal muscle[32] and the activation of p38αβ MAPK signaling by FGFR1 prompted us to compare FGFR1 activation and signaling in aged versus young SCs (Supplementary Fig. 5). Phospho-FGFR$^+$ (pFGFR$^+$) SC numbers were reduced in aged cultures at 24 h post-isolation compared to young cultures (Fig. 4a,b) where inhibition of FGFR1 signaling reduced p38αβ MAPK signaling only in young SCs (Fig. 4c). FGF signaling was then examined by single cell analyses using Sdc4 as an SC marker (Fig. 4d) to detect p38αβ MAPK protein (Fig. 4e) in SCs isolated from equivalent muscle masses. Addition of FGF-2 stimulated p38αβ MAPK phosphorylation in young SCs but not in aged SCs (Fig. 4f). Inhibition of FGF signaling with SU5402 eliminated FGF-stimulated phosphorylation of p38αβ MAPK in young SCs but had no effect on aged SCs (Fig. 4g), highlighting the FGF insensitivity of p38αβ MAPK in aged SCs. We next tested whether inhibiting FGFR signaling with SU5402 affected self-renewal as assayed by CFDA-SE label retention (Fig. 4h). The number of young but not aged label-retaining Pax7$^+$ cells were significantly decreased by inhibition of FGFR signaling (Fig. 4i).

The insensitivity of aged SCs to FGF-2 and and their elevated p38αβ MAPK activity coupled with the reported upregulation of FGF-2 in aged muscle[32] suggest that aged muscle is compensating for attenuated SC FGFR1 signaling. Therefore, we utilized an inducible, constitutively active FGFR1 (iFR1)[38,39] to provide ligand-independent FGFR1 signaling via small molecule-induced dimerization[38]. Upon isolation, myofiber-associated SCs were transfected with iFR1 expression vectors, treated with Dimerizer B/B to activate iFR1[38,39], harvested at 72 h for immunofluorescence analysis (Fig. 5a), and iFR1$^+$ SCs scored for Pax7 and Myogenin (Fig. 5b). In the absence of iFR1 dimerization, Myogenin$^+$ cells predominated aged SC cultures, while Pax7$^+$ cells were more prevalent in young cultures (Fig. 5c). Activation of iFR1 increased Pax7$^+$ cells at the expense of Myogenin$^+$ cells in both aged and young cultures, where nearly all SCs were Pax7$^+$ following iFR1 activation (Fig. 5c). Accompanying the increase in Pax7$^+$ cells was a subcellular re-localization of phospho-FGFR and iFR1 (Fig. 5d,e). The diffuse distribution of iFR1 became localized and asymmetric upon receptor activation (Fig. 5f). Moreover, upon iFR1 activation, the majority

of phospho-p38αβ MAPK (Fig. 5e,f) co-localized asymmetrically with iFR1 in young as well as aged SCs (Fig. 5f). A CFDA-SE dye retention assay (Fig. 5g) identified self-renewed, quiescent young and aged SCs following iFR1 activation (Fig. 5h). Addition of Dimerizer B/B or FGF-2 yielded similar numbers of CFDA-SE$^+$ label-retaining cells in young cultures (Fig. 5i), indicating equivalent SC self-renewal from ectopic iFR1 signaling or FGF-2 addition in young SCs (Fig. 5j). In contrast, iFR1 activation but not FGF-2 addition increased self-renewal of aged SCs identified as Pax7$^+$ CFDA-SE label-retaining SCs (Fig. 5i,j).

Ectopic activation of FGFR1 signaling via iFR1 and partial inhibition of p38αβ MAPK in aged satellite cells restore asymmetric localization of phospho-p38αβ MAPK, partially rescuing self-renewal in culture, suggesting both treatments should enhance aged SC engraftment. Since it is not feasible to test iFR1 activation in transplantation assays because the iFR1 transfections are transient and the levels of Dimerizer B/B and dosing *in vivo* have not been determined, we transplanted aged SCs and young SCs pretreated with 10 μM SB203580. Freshly isolated myofibers with associated SCs from young and aged β*ActGFP* mice were incubated in DMSO carrier or 10 μM SB20350 for 12 h and then transplanted into young host muscles with $BaCl_2$ to elicit a muscle injury (Fig. 6a). Thirty days post-injection, muscles were harvested and donor SCs identified by c-Met immunostaining and GFP fluorescence (Fig. 6b). The presence or absence of SB203580 had no significant effect on young donor SC engraftment, but pretreatment of aged donor SCs with 10 μM SB203580 restored aged SC engraftment to that observed for young donor SCs 30 d post-injection (Fig. 6c).

Discussion

Skeletal muscle function and mass decline with age beginning around age 40 in men[40]. Sarcopenia, a more severe loss of muscle mass and function, leads to frailty, increased morbidity and increased health care costs[2,4,5]. The mechanisms involved in sarcopenia are only beginning to be understood but clearly involve major metabolic changes in muscle tissue[41] and reductions in skeletal muscle regeneration[6,7,9]. Previous work has demonstrated that an altered global environment in aged mice inhibited SC function and suggested that aged SCs could be completely rescued simply by exposure to a young environment[18-22]. The present study aimed to address two major unresolved issues: 1) whether aged SCs exhibit cell intrinsic alterations in self-renewal and 2) the long-term behavior of aged SCs transplanted to a young environment. We found that aged SCs fail to self-renew even when transplanted into a young host environment. The failure of the young environment to rescue aged SC self-renewal led to the identification of cell-autonomous deficits in aged SC self-renewal where alterations in an FGF/p38αβ MAPK signaling pathway appear at the core of these age-associated deficits.

Elevated p38αβ MAPK activity is present in freshly isolated aged SCs when compared to young SCs. Accompanying the elevated p38αβ MAPK signaling is an attenuation of FGFR1 stimulation by FGF ligands. Thus, the aged environment is likely responsible for the elevated signaling of phospho-p38, possibly from increased cellular stress and inflammatory responses. We propose that the aged environment contributes to elevated p38αβ MAPK

activity in aged SCs, and furthermore, that hyperactive p38αβ MAPK prevents asymmetric p38αβ MAPK signaling, thus disrupting asymmetric division and the generation of quiescent daughter cells (Fig. 6d). The observations that partial inhibition of p38αβ MAPK signaling restores (i) generation of $Pax7^+$ cells, (ii) asymmetric phospho-p38αβ MAPK, (iii) increases aged SC self-renewal by 3-fold, and (iv) rescues aged SC engraftment and maintenance in young host muscle, strongly supports this model. Near complete inhibition of p38αβ MAPK virtually eliminates self-renewal, demonstrating that p38αβ MAPK is required for SC self-renewal[42]. Other published work demonstrates that elevated p38αβ MAPK signaling promotes myoblast differentiation[39,40], which may exacerbate the failure of aged SCs to expand irrespective of the surrounding environment. Together, these data support a critical role for p38αβ MAPK in SC self-renewal, suggesting that the subcellular localization, duration of signaling, and timing of p38αβ MAPK activation are highly regulated to permit asymmetric division and SC self-renewal.

While the role of FGFR1 in regulating SC self-renewal is less clear, prior observations that loss of FGFR1 signaling *in vivo* reduces skeletal muscle mass during development[29], that FGFR1 is expressed in freshly isolated SCs[37], and that FGFR1 signaling represses myogenesis in satellite cell-derived cell lines[28], suggest that FGFR1 signaling plays an important role in regulating satellite cell function. Here we show that ectopic, ligand-independent activation of FGFR1 signaling restores asymmetric phospho-p38αβ MAPK activation, consistent with the rescue of aged SC self-renewal in culture. Moreover, activation of ectopically expressed iFR1 promotes asymmetric co-localization of iFR1 and phospho-p38αβ MAPK, supporting a role for FGFR1 signaling in asymmetric SC division and self-renewal (Fig. 6d). Our data are consistent with a role for FGFR1 in organizing an asymmetric signaling complex[33], which then functions to asymmetrically activate p38αβ MAPK (Fig. 6d). Consistent with this hypothesis are observations that FGFR1 signaling is disrupted in *Sdc4* null mice[43], and that *Sdc4* null SCs fail to engraft and expand when transplanted into wild-type muscle[23]. The attenuation of FGFR1 activation by FGF ligands in aged SCs prevents asymmetric division, promoting lineage commitment in both daughter cells and reducing self-renewal and thus, reducing the stem cell population (Fig. 6d).

The attenuation of intracellular responses initiated by extracellular FGF-2 in aged SCs could arise from changes in either FGFR1 interactions with other cell surface proteins or from altered heparan sulfate since FGF binding and signaling from FGFR1 requires a ternary complex comprising heparan sulfate, FGFR1 and the FGF ligand[44-46]. Thus, alterations in either FGFR1 or heparan sulfate, observed in other aging tissues[47,48], could contribute to the decline in signal transduction efficiency and the cell autonomous loss of SC self-renewal. Consistent with this idea is the observation that FGF-2 increases in aged muscle[32], which could be a compensatory response. Since ligand-independent activation of FGFR1 restored SC self-renewal, it seems likely that downstream FGFR1 signaling remains functional and responsive in aged SCs. While the precise mechanism of FGFR1 involvement in asymmetric activation of p38αβ MAPK is unclear, it is an area primed for future investigation. Manipulating stem cell self-renewal by enhancing FGFR1 signaling and reducing p38αβ MAPK activation to increase SC self-renewal represent potentially new therapeutic targets for improving skeletal muscle regeneration and maintenance in the aged.

Methods

Animal Studies

Animal experiments in this study were performed in accordance with protocols approved by the Institutional Animal Care and Use Committee at the University of Colorado. Female C57BL/6 mice (Jackson Labs and the National Institutes on Aging) were used for all *ex vivo* experiments. Transplant recipients were female C57Bl/6xDBA2 mice (Jackson Labs) while donor tissue was isolated from female, β-actin GFP (FVB.Cg-Tg(CAG-EGFP)B5Nagy/J; Jackson Labs) mice referred to as β*ActGFP*[23], with sample size determined by power analysis of previous transplantation studies. Mice were used at 3–6 months of age (Young, median 4 months) or 20–25 months of age (Aged, median 23 months). β*ActGFP* mice were aged in our facilities for transplantation assays.

Cell Isolation, Culture and Transfection

Myofibers with associated SCs were isolated for immediate use as previously described[33]. For all experiments, myofibers were cultured in growth medium, F12-C (Life Science Products) + 15% horse serum ± 1.5 nM FGF-2 at 6% O_2 with daily medium and reagent changes. CFDA-SE (Invitrogen) was used at 10 μM, SU5402 (Tocris) at 25 μM, SB203580 (Tocris) at 10 and 25 μM, BIRB 796 (Millipore) at 10 μM, UO126 at 10 μM (AG Scientific), and Dimerizer B/B at 100 μM (B/B Homodimerizer, previously AP20187, Clontech). Sodium orthovanadate was used at 2 mM (Sigma Aldrich) during fixation in phosphorylation experiments. Dimethyl sulfoxide (DMSO) was used as control for inhibitor treatment.

For AraC experiments, myofibers were cultured for 72 h then incubated with or without 100 μM AraC (Sigma Aldrich) for 48 h and fixed (Day 5). The remaining myofibers were washed with growth medium and cultured for an additional 72 h without AraC (Day 8, AraC Recovery).

For transfection experiments, we purchased the plasmid pSH1/M-FGFR1-Fv-FVl2-E containing the inducible iFGFR1 construct from Addgene (Addgene plasmid 15285)[49]. We transfected the iFGFR1 construct or performed a mock transfection into myofiber-associated SCs with Lipofectamine 2000 (Invitrogen) 8 h post-isolation. Dimerizer B/B was added 24 h post-transfection, and added with daily media changes until fixation at 48 h or 72 h.

For CFDA-SE retention assays, myofiber-associated cells were either cultured in growth media or transfected as above and treated with Dimerizer B/B or FGF-2 after 24 h. At 48 h, CFDA-SE in Dulbecco's PBS was added for 15 min then myofibers were washed three times with growth media to remove excess CFDA-SE. For each experiment, a subset of myofibers was fixed 30 min post-CFDA-SE treatment to verify CFDA-SE uptake by all Syndecan-4$^+$ SCs. The remaining myofibers were transferred to growth media (with FGF-2 or Dimerizer B/B for iFGFR1 transfection experiments) and fixed at 72 h.

Myofiber Transplantation

For heterochronic local transplantation assays, SCs from β*ActGFP* mice were isolated alongside myofibers from wild-type mice. Cells were preplated (2–3 h) on an uncoated plate during myofiber isolation. A total of 2×10^4 cells were mixed with 50 myofibers in a 0.2 mL microcentrifuge tube in 0.2 mL warm growth media containing 1.5 nM FGF-2. The mixture was rotated slowly at 37 °C for 3.5 h, then myofibers were transferred to individual tissue culture plates for three successive washes with fresh growth media to remove unattached cells, and cultured for 24 or 72 h as described above.

Transplantation of myofiber-associated SCs to host *tibialis anterior* muscles was performed as previously described[23] except that myofibers were pretreated for 5 h with 1.5 nM FGF-2 or overnight with 10 μM SB203580 or FGF-2 prior to injection. Five to seven myofibers were transplanted (Supplementary Fig. 1) to recipient mice with recipients randomly selected from a group of young C57BL/6 mice. *Tibialis anterior* muscles were harvested and sections processed as previously described[23]. To count the number of donor SCs, >10 fields (750 μm × 750 μm) were scored across serial 10 μm sections from mid-muscle. The range in reported sample size is due to attrition of mice between injury and harvest.

Flow cytometry and analysis

For phosphorylation analysis, SCs were isolated and cultured in growth media with 25 μM SU5402 (Tocris) or DMSO on uncoated plates for 16 h (starved of FGF-2). Additional SU5402 or DMSO and 2mM sodium orthovanadate were added 1 h before FGF-2 stimulation. Cells were treated with or without FGF-2 in Bovine Serum Albumin (BSA) for 5 min then fixed in 4% paraformaldehyde at 4 °C, remaining at 4 °C throughout flow cytometry analysis. Sodium orthovanadate (Sigma Aldrich) was added to all reagents during primary antibody staining. Cells were permeabilized with 0.1% Triton X-100 then washed and blocked in 2% Fetal Bovine Serum (FBS). Cells (excluding unlabelled controls) were stained with 1:1000 chicken anti-Syndecan-4 and 1:50 mouse anti-phospho-p38 MAPK (Cell Signaling 9216S) for 1 h in 2% FBS in PBS, then 30 min with secondary antibodies (anti-chick AlexaFluor 647 and anti-mouse AlexaFluor 488), and stained before analysis with 4′,6-diamidino-2-phenylindole (DAPI). Cells were analyzed by flow cytometry (CyAN ADP Analyzer) and data analyzed in FlowJo 9.6. A gate was set to exclude small debris based off previous analysis of freshly isolated SCs. Population shifts in Syndecan-4^+/phospho-$p38^+$ cells were quantified by population comparison (Overton subtraction) in FlowJo.

Immunofluorescence

All cells and tissues were fixed in 4% paraformaldehyde and permeabilized as necessary with 0.1% Triton X-100. Muscle sections were prepared as previously described[23,37]. All slides were blocked in 3% BSA 1 h at RT and stained in 1% BSA. Primary antibodies were incubated at 4 °C overnight, and secondary antibodies incubated 1 h at RT. DAPI staining was used to mark nuclei. The following primary antibodies were used: chicken Syndecan-4 (1:500)[37], chicken Syndecan-3 (1:50)[37], mouse Pax7 (Developmental Hybridoma Bank at Iowa University, 1:5), rabbit MyoD (C-20, Santa Cruz Biotechnology, sc-304, 1:400), mouse Myogenin (F5D, Developmental Hybridoma Bank at Iowa University, straight),

rabbit p38 MAPK (C-20, Santa Cruz Biotechnology, sc-535, 1:50), mouse phospho-p38 MAPK (Cell Signaling, 9216S, 1:50), rabbit phospho-FGFR (Cell Signaling, 3471S, 1:50), rat HA tag (used to image iFGFR1 transfected cells; Roche, 11867423001, 1:200), rabbit c-Met (Invitrogen 718000, 1:200) rat Laminin (Sigma, L0663, 1:200). AlexaFluor 488-, 555-, and 647-conjugated secondary antibodies (Invitrogen) were used at 1:500.

Microscopy and Image Processing

A Leica TCS SP2 AOBS confocal microscope with Leica software, using an HC Plan Apochromat 20x/0.70 IMM CORR CS lens was used to image most muscle sections. A Zeiss 510 confocal microscope with Zen software, using a Plan-Apochromat 63x/1.40 lens, was used to image SB203580-treated and control transplant sections. Micrographs of local transplantation assays were captured with a Nikon Eclipse E800 equipped with a Sensicam (Cooke) digital camera and Slidebook v4.1 (3i) software with a PlanFluor 20x/NA 0.50 PH1 DLL (Nikon) lens. All other myofiber experiments were imaged with a Leica DM RXA Spinning Disk confocal microscope with EM-CCD digital camera (Hamamatsu) with Metamorph software (Molecular Devices), using HC Plan APO 20x/0.70 or HCX PL APO 40x/0.85 CORR lenses. All digital microscopic images were acquired at room temperature. The mounting medium for cells and sections was Vectashield Mounting Medium (Vector). Images were processed then scored with blinding in ImageJ64. As necessary, the brightness and contrast were adjusted linearly for the entire image and adjusted equivalently across the experimental image set. Muscle section images are averaged Z-stacks with Tikhonov-Miller deconvolution (ImageJ64) of the Syndecan-4, c-Met and Laminin channels.

Microarray and Analysis

Raw data was pre-processed using Genespring software (Agilent) and analyzed for differential gene expression changes occurring over time. For heat maps, individual probeset expression (log2) was normalized to the mean relative expression (log2) of all transcript probesets to one gene across both ages. In the Affymetrix 430 v.2 mouse microarray, there may be multiple probesets corresponding to different transcripts from a single gene; this is indicated by repeated transcript names in the figures and table. All microarray data has been deposited in the NCBI Gene Expression Omnibus (GEO) and can be accessed using GEO ID 200047104.

Statistical analysis

All values represent the mean ± s.e.m. of at least three biological replicates except microarray data, which represent biological replicates from SCs isolated from multiple animals. Statistical differences between groups were determined by unpaired, two-tailed Student's *t*-test, one-way ANOVA with Tukey's post-hoc test or two-way ANOVA with Tukey's post-hoc test using Graph-Pad Prism 6. $P < 0.05$ was determined to be significant for all experiments. *P* values for signaling networks were determined by IPA software. Actual *P* values and specific statistical tests are listed in each figure legend.

Supplementary Material

Refer to Web version on PubMed Central for supplementary material.

Acknowledgments

The Olwin lab members especially B. Pawlikowski, M. Hall and A. Cadwallader for revising the manuscript and helpful discussions. T. Vogler, T. McClure and M. Palmer for technical assistance. N. Dalla Betta helped with mouse maintenance. C. English and the CU-Boulder MCDB Light Microscopy Core provided facilities and assistance. D.M Spencer developed the iFGFR1 construct available from Addgene. The National Institutes on Aging for making aging mouse lines available. This work was supported by grants from the National Institutes of Health (AR49446 and AG040074) and The Ellison Medical Foundation to B.B.O., and from the National Institutes of Health (T32GM007135) to J.D.B.

References

1. Evans WJ, Campbell WW. Sarcopenia and age-related changes in body composition and functional capacity. 1993; 123:465–468.
2. Baumgartner RN, et al. Epidemiology of sarcopenia among the elderly in New Mexico. 1998; 147:755–763.
3. Roubenoff R. Sarcopenia: A major modifiable cause of frailty in the elderly: Sarcopenia in aging. 2000; 4:140–142.
4. Landi F, et al. Sarcopenia and mortality risk in frail older persons aged 80 years and older: results from ilSIRENTE study. 2013; 42:203–9.10.1093/ageing/afs194
5. Janssen I, Shepard DS, Katzmarzyk PT, Roubenoff R. The healthcare costs of sarcopenia in the United States. 2004; 52:80–5.
6. Brooks SV, Faulkner JA. Contraction-induced injury: recovery of skeletal muscles in young and old mice. 1990; 258:C436–C442.
7. Grounds MD. Age-associated changes in the response of skeletal muscle cells to exercise and regeneration. 1998; 854:78–91. doi:9928422.
8. Karakelides H, Nair KS. Sarcopenia of aging and its metabolic impact. 2005; 68:123.
9. Day K, Shefer G, Shearer A, Yablonka-Reuveni Z. The depletion of skeletal muscle satellite cells with age is concomitant with reduced capacity of single progenitors to produce reserve progeny. 2010; 340:330–43.10.1016/j.ydbio.2010.01.006
10. Mauro A. Satellite cell of skeletal muscle fibers. 1961; 9:493–5.
11. Sambasivan R, et al. Pax7-expressing satellite cells are indispensable for adult skeletal muscle regeneration. 2011; 138:3647–56.10.1242/dev.067587
12. Lepper C, Partridge TA, Fan CM. An absolute requirement for Pax7-positive satellite cells in acute injury-induced skeletal muscle regeneration. 2011; 138:3639–46.10.1242/dev.067595
13. Murphy MM, Lawson JA, Mathew SJ, Hutcheson DA, Kardon G. Satellite cells, connective tissue fibroblasts and their interactions are crucial for muscle regeneration. 2011; 138:3625–37.10.1242/dev.064162
14. Sadeh M. Effects of aging on skeletal muscle regeneration. 1988; 87:67–74.
15. McGeachie J, Grounds M. Retarded myogenic cell replication in regenerating skeletal muscles of old mice: an autoradiographic study in young and old BALBc and SJL/J mice. 1995; 280:277–282.
16. Marsh DR, Criswell DS, Carson JA, Booth FW. Myogenic regulatory factors during regeneration of skeletal muscle in young, adult, and old rats. 1997; 83:1270–1275.
17. Conboy IM, Conboy MJ, Smythe GM, Rando TA. Notch-mediated restoration of regenerative potential to aged muscle. 2003; 302:1575–7.10.1126/science.1087573
18. Collins CA, Zammit PS, Ruiz AP, Morgan JE, Partridge TA. A population of myogenic stem cells that survives skeletal muscle aging. 2007; 25:885–94.10.1634/stemcells.2006-0372
19. Carlson BM, Faulkner JA. Muscle transplantation between young and old rats: age of host determines recovery. 1989; 256:C1262–C1266.
20. Carlson BM, Faulkner JA. The Regeneration of Noninnervated Musele Grafts and Marcaine-Treated Muscles in Young and Old Rats. 1996; 51:B43.
21. Conboy IM, Conboy MJ, Wagers AJ, Girma ER, Weissman IL, Rando TA. Rejuvenation of aged progenitor cells by exposure to a young systemic environment. 2005; 433:760–4.

22. Brack AS, Rando TA. Intrinsic changes and extrinsic influences of myogenic stem cell function during aging. 2007; 3:226–37.
23. Hall JK, Banks GB, Chamberlain JS, Olwin BB. Prevention of muscle aging by myofiber-associated satellite cell transplantation. 2010; 2:57ra83.10.1126/scitranslmed.3001081
24. Hannon K, Kudla AJ, McAvoy MJ, Clase KL, Olwin BB. Differentially expressed fibroblast growth factors regulate skeletal muscle development through autocrine and paracrine mechanisms. 1996; 132:1151–9.
25. Sheehan SM, Allen RE. Skeletal muscle satellite cell proliferation in response to members of the fibroblast growth factor family and hepatocyte growth factor. 1999; 181:499–506.
26. Kastner S, Elias MC, Rivera AJ, Yablonka-Reuveni Z. Gene expression patterns of the fibroblast growth factors and their receptors during myogenesis of rat satellite cells. 2000; 48:1079–96.
27. Lagha M, et al. Pax3 regulation of FGF signaling affects the progression of embryonic progenitor cells into the myogenic program. 2008; 22:1828–37.10.1101/gad.477908
28. Kudla AJ, Jones NC, Rosenthal RS, Arthur K, Clase KL, Olwin BB. The FGF receptor-1 tyrosine kinase domain regulates myogenesis but is not sufficient to stimulate proliferation. 1998; 142:241–50.
29. Flanagan-Steet H, Hannon K, McAvoy MJ, Hullinger R, Olwin BB. Loss of FGF receptor 1 signaling reduces skeletal muscle mass and disrupts myofiber organization in the developing limb. 2000; 218:21–37.10.1006/dbio.1999.9535
30. Jones NC, Fedorov YV, Rosenthal RS, Olwin BB. ERK1/2 is required for myoblast proliferation but is dispensable for muscle gene expression and cell fusion. 2001; 186:104–15.10.1002/1097-4652(200101)186:1<104::AID-JCP1015>3.0.CO;20
31. Jones NC, et al. The p38{alpha}/{beta} MAPK functions as a molecular switch to activate the quiescent satellite cell. 2005; 169:105–16.10.1083/jcb.200408066
32. Chakkalakal JV, Jones KM, Basson MA, Brack AS. The aged niche disrupts muscle stem cell quiescence. 201210.1038/nature11438
33. Troy A, Cadwallader AB, Fedorov Y, Tyner K, Tanaka KK, Olwin BB. Coordination of Satellite Cell Activation and Self-Renewal by Par-Complex-Dependent Asymmetric Activation of p38α/β. MAPK. 2012; 11:541–53.10.1016/j.stem.2012.05.025
34. Kang JS, et al. A Cdo-Bnip-2-Cdc42 signaling pathway regulates p38alpha/beta MAPK activity and myogenic differentiation. 2008; 182:497–507.10.1083/jcb.200801119
35. Gillespie MA, et al. p38-{gamma}-dependent gene silencing restricts entry into the myogenic differentiation program. 2009; 187:991–1005.10.1083/jcb.200907037
36. Shefer G, Van de Mark DP, Richardson JB, Yablonka-Reuveni Z. Satellite-cell pool size does matter: defining the myogenic potency of aging skeletal muscle. 2006; 294:50–66.10.1016/j.ydbio.2006.02.022
37. Cornelison DD, Filla MS, Stanley HM, Rapraeger AC, Olwin BB. Syndecan-3 and syndecan-4 specifically mark skeletal muscle satellite cells and are implicated in satellite cell maintenance and muscle regeneration. 2001; 239:79–94.10.1006/dbio.2001.0416
38. Whitney ML, Otto KG, Blau CA, Reinecke H, Murry CE. Control of myoblast proliferation with a synthetic ligand. 2001; 276:41191–6.10.1074/jbc.M103191200
39. Stevens KR, et al. Chemical dimerization of fibroblast growth factor receptor-1 induces myoblast proliferation, increases intracardiac graft size, and reduces ventricular dilation in infarcted hearts. 2007; 18:401–12.10.1089/hum.2006.161
40. Faulkner JA, Larkin LM, Claflin DR, Brooks SV. Age-related changes in the structure and function of skeletal muscles. 2007; 34:1091–1096.
41. Rüegg MA, Glass DJ. Molecular mechanisms and treatment options for muscle wasting diseases. 2011; 51:373–95.10.1146/annurev-pharmtox-010510-100537
42. Brien P, Pugazhendhi D, Woodhouse S, Oxley D, Pell JM. P38α MAPK Regulates Adult Muscle Stem Cell Fate By Restricting Progenitor Proliferation During Postnatal Growth And Repair. 201310.1002/stem.1399
43. Cornelison DD, Wilcox-Adelman SA, Goetinck PF, Rauvala H, Rapraeger AC, Olwin BB. Essential and separable roles for Syndecan-3 and Syndecan-4 in skeletal muscle development and regeneration. 2004; 18:2231–6.10.1101/gad.1214204

44. Yayon A, Klagsbrun M, Esko J, Leder P, Ornitz D. Cell surface, heparin-like molecules are required for binding of basic fibroblast growth factor to its high affinity receptor. 1991; 64:841–848.

45. Rapraeger AC, Krufka A, Olwin BB. Requirement of heparan sulfate for bFGF-mediated fibroblast growth and myoblast differentiation. 1991; 252:1705–8.

46. Schlessinger J, et al. Crystal structure of a ternary FGF-FGFR-heparin complex reveals a dual role for heparin in FGFR binding and dimerization. 2000; 6:743–50.

47. Huynh MB, et al. Age-related changes in rat myocardium involve altered capacities of glycosaminoglycans to potentiate growth factor functions and heparan sulfate-altered sulfation. 2012; 287:11363–73.10.1074/jbc.M111.335901

48. Williamson KA, et al. Age-related impairment of endothelial progenitor cell migration correlates with structural alterations of heparan sulfate proteoglycans. 2013; 12:139–47.10.1111/acel.12031

49. Welm BE, Freeman KW, Chen M, Contreras A, Spencer DM, Rosen JM. Inducible dimerization of FGFR1 development of a mouse model to analyze progressive transformation of the mammary gland. 2002; 157:703–714.

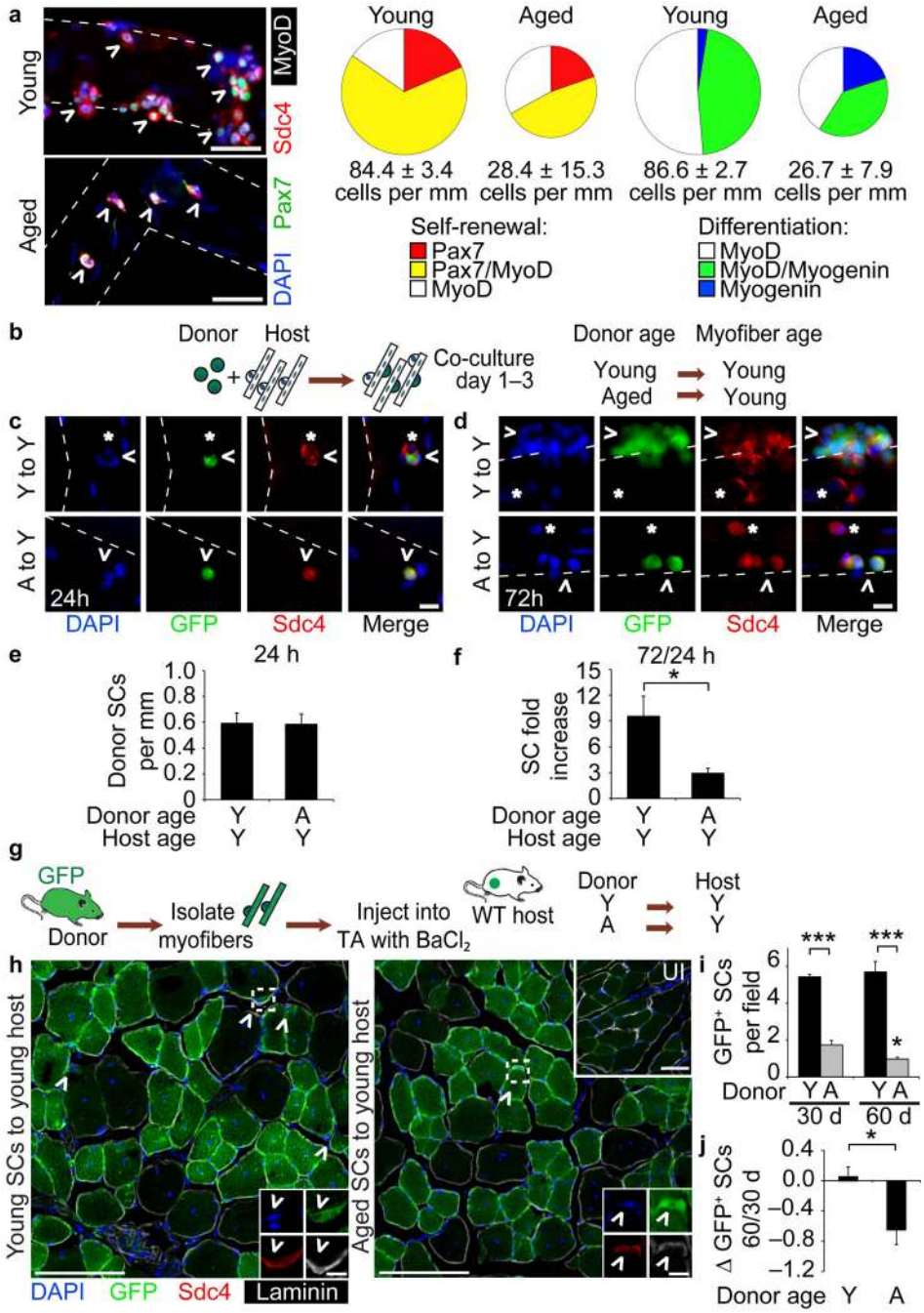

Figure 1. Heterochronic transplantation of aged satellite cells (SCs) to local or systemic young environment fails to rescue age-associated phenotypes

(**a**) (left) Young and aged myofiber-associated SCs cultured for 96 h and stained with Pax7, MyoD and Myogenin. Scale bar, 50 μm. (right) Percentages of Syndecan-4$^+$ (Sdc4$^+$) SCs at 96 h that are quiescent (Pax7$^+$), proliferating myoblasts (Pax7$^+$/MyoD$^+$ or MyoD$^+$) or differentiating myocytes (MyoD$^+$/Myogenin$^+$ or Myogenin$^+$). Chart area scaled to Sdc4$^+$ SCs per myofiber length (n = 3, ≥20 myofibers/condition. $P < 0.05$ for 96 h Young vs. Aged cells/myofiber length and Pax7$^-$/MyoD$^+$. $P < 0.001$ for MyoD$^-$/Myogenin$^+$, *t*-test.).

(**b–f**) (**b**) Schematic for heterochronic, *βActGFP* SC and wild-type myofiber co-culture. GFP^+Sdc4^+ SCs (^) and endogenous $Sdc4^+$ SCs (*) after (c) 24 h or (d) 72 h in culture. Scale bar, 50 μm. Average number of $GFP^+/Sdc4^+$ SCs per myofiber length at (e) 24 h, and (f) fold increase in donor SCs per myofiber at 72 h in culture (n = 3, ≥20 myofibers per condition. *$P < 0.05$, t test). (**g-j**) (**g**) Schematic for heterochronic myofiber transplantation to young muscle hosts. (**h**) Muscle sections harvested at 30 d or 60 d (not shown) post-transplantation . Insets depict donor-derived SCs (^ = $GFP^+/Sdc4^+$) and contralateral, uninjured (UI) muscle. Scale bars, 50 μm or 5 μm (SCs). (i) Average number of donor-derived SCs per field (**j**) and Log_2 fold-change in donor-derived SCs per field comparing 60 d vs. 30 d post-transplantation ($n = 3$ to 5 transplant recipients. *$P < 0.05$ for Aged 30 d vs. 60 d; ***$P < 0.001$ for Young vs. Aged, *t* test). Mean ± s.e.m. for all.

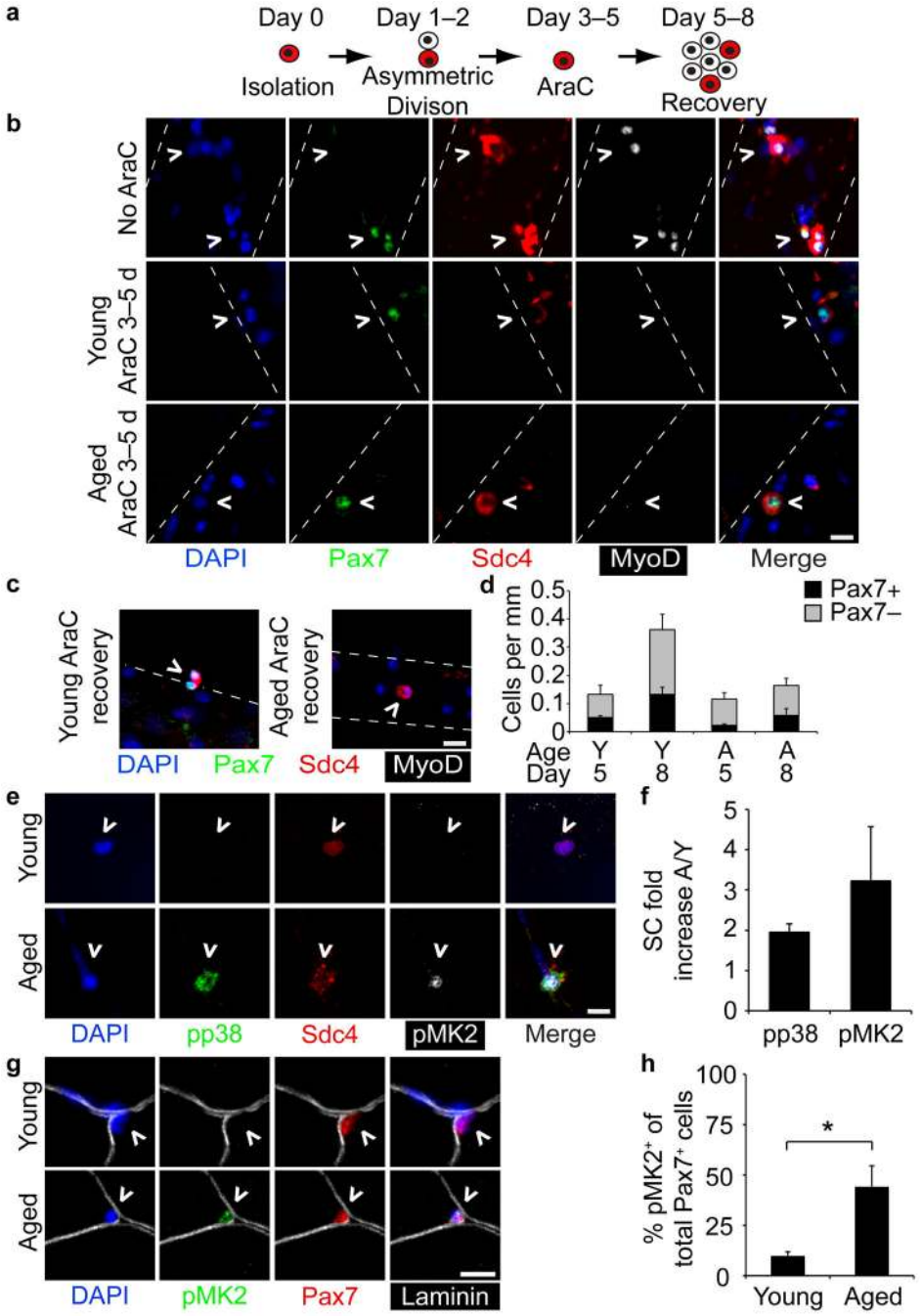

Figure 2. Loss of self-renewal in aged SCs correlates with elevated p38 signaling in aged SCs

(**a–d**) (**a**) Schematic for AraC treatment of myofibers to identify quiescent daughter SCs. (**b**) Young and aged myofibers treated for 48 h with or without AraC (Day 5) and (**c**) after additional 72 h recovery without AraC (Day 8). Scale bars,10 μm. (**d**) Average number of Pax7^{+}, AraC-resistant SCs (^) and Pax7^{-}, terminally differentiated myocytes per myofiber length ($P < 0.05$ for Pax7^{+} Young 5 d vs. 8 d and total cells Young 5 d vs. 8 d, one-way ANOVA. ≥20 myofibers scored/condition). (**e-h**) young and aged (**e**) Sdc4^{+} myofiber-associated SCs (^) at 1 h post-dissection stained for phospho-p38 (pp38) and phospho-MK2

(pMK2) (aged SC is adjacent to myonucleus) and plotted (**f**) for the average fold increase in number of $pp38^+$ and $pMK2^+$ aged SCs/young SCs (≥20 myofibers scored/age). (**g**) $Pax7^+$ SCs (^) in young and aged uninjured muscle sections stained for pMK2 and Pax7 (Scale bars, 10 μm) and plotted for (**h**) the percentage of activated SCs ($Pax7^+/pMK2^+$)/total SCs ($Pax7^+$) (≥30 fields. $*P < 0.05$, t test). Mean ± s.e.m. and $n = 3$ for all.

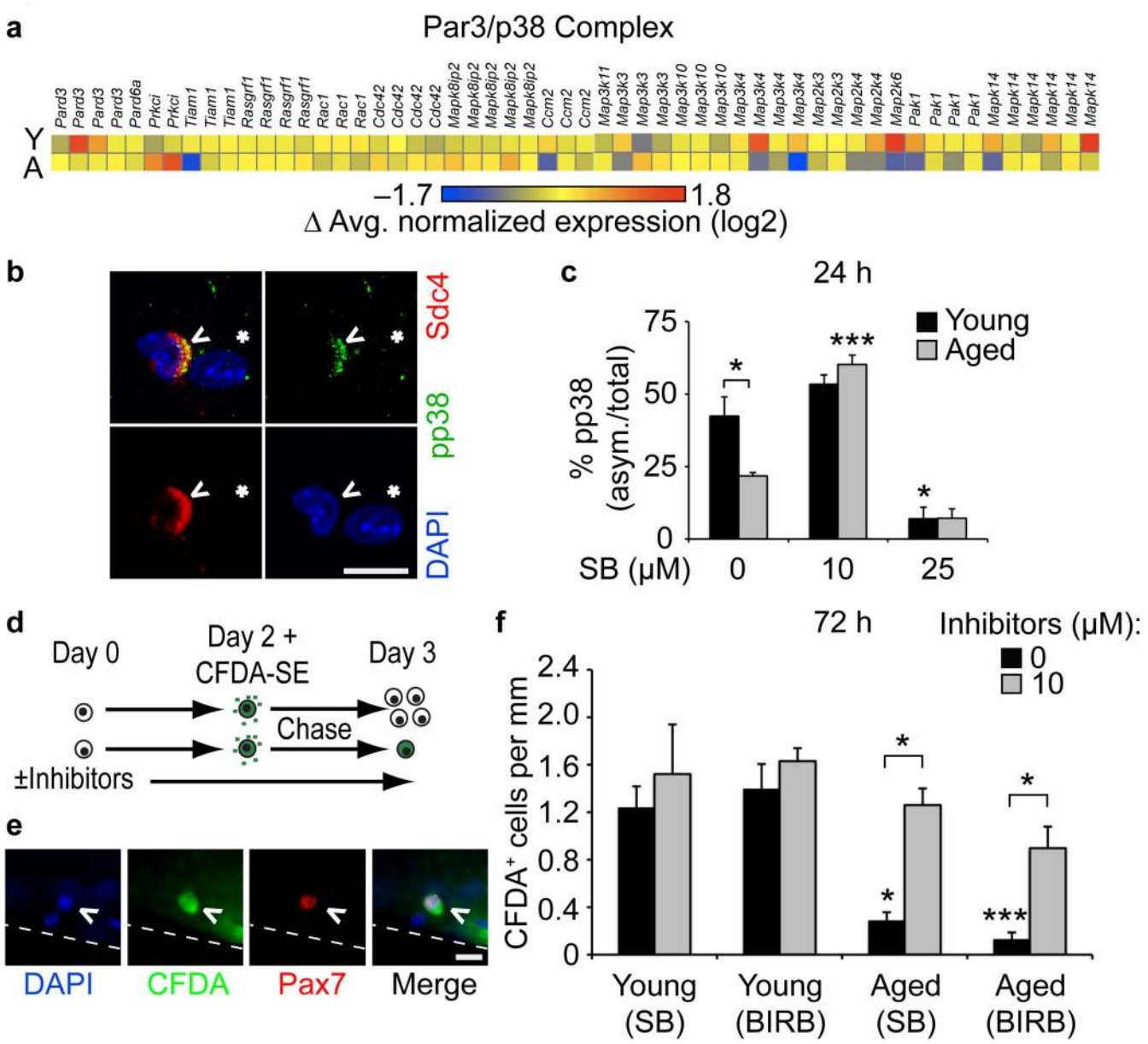

Figure 3. Partial inhibition of p38αβ MAPK rescues aged SCs self-renewal

(**a**) Heatmap of normalized expression of proteins involved in asymmetric SC cell division. (**b–c**) (**b**) Myofiber-associated, asymmetric phospho-p38$^+$ SC (^) near a myonucleus (*). Scale bar, 10 μm. (c) Percentage of asymmetric (asym.) phospho-p38$^+$ SCs after 24 h culture treated with increasing SB203580 (SB) (*P < 0.05 for Young vs. Aged 0 μM SB, Young 0 vs. 25 μM SB; ***P < 0.001 for Aged 0 vs. 10 μM SB, (unmarked) Young 10 vs. 25 μM SB and Aged 10 vs. 25 μM SB, two-way ANOVA. Mean ± s.e.m., n = 3 experiments, ≥20 myofibers/condition). (**d–f**) (**d**) Schematic for CFDA-SE retention assay. (**e**) Self-renewed (Pax7$^+$/CFDA-SE$^+$), myofiber-associated SC. Scale bar, 10 μm. Scored and plotted (**f**) as average number of Pax7$^+$/CFDA-SE$^+$ SCs per myofiber length either untreated or treated with SB203580 or BIRB 796 (*P < 0.05 for Young vs. Aged 0 μM SB, Aged 0 vs. 10 μM

(SB and BIRB); ***$P < 0.001$ for Young vs. Aged 0 μM BIRB, two-way ANOVA; mean ± s.e.m., $n = 3$ experiments, ≥30 myofibers).

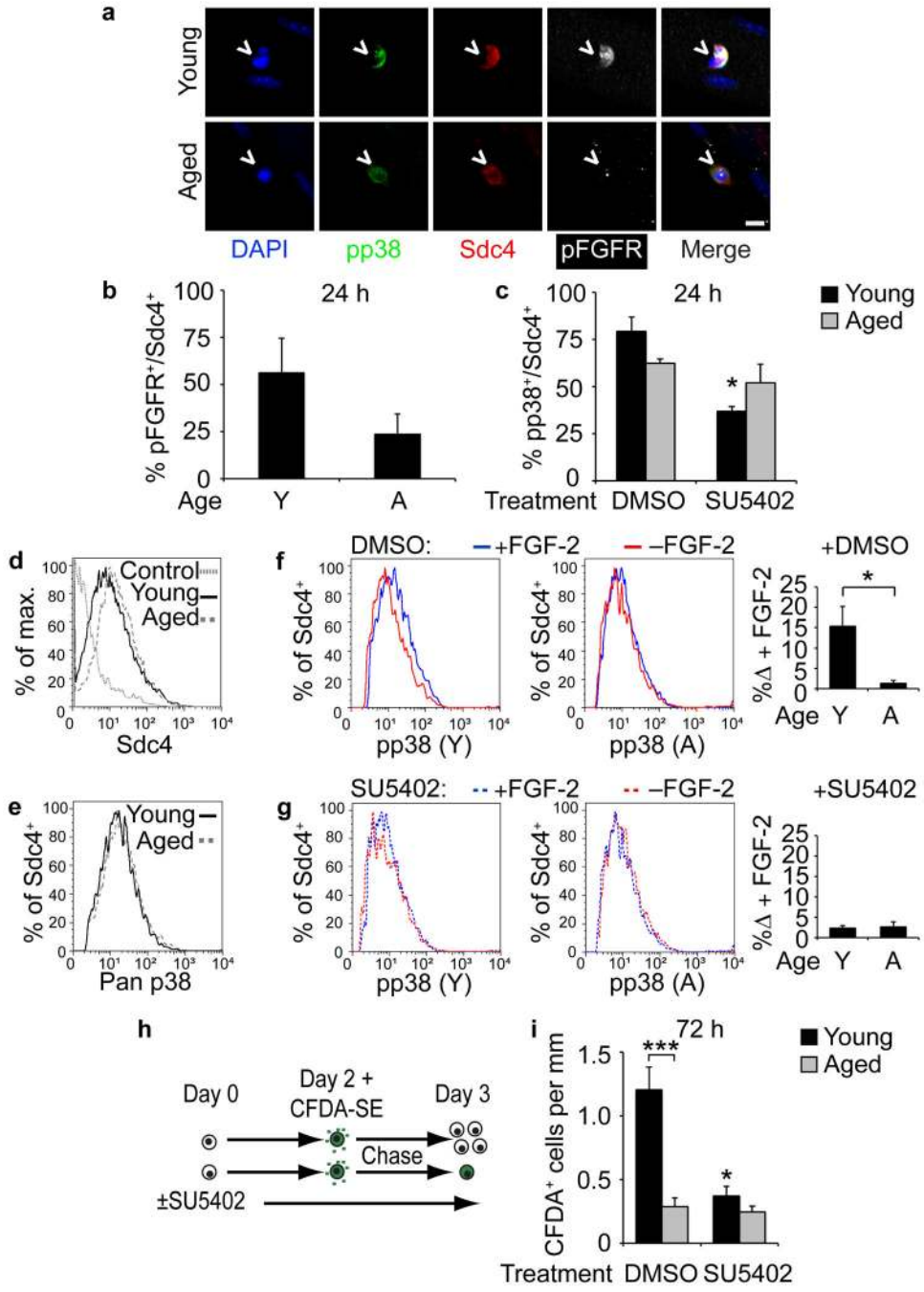

Figure 4. FGFR1 signaling is altered in aged compared to young SCs

(**a–c**) (**a**) Young and aged Sdc4$^+$ myofiber-associated SCs (^) cultured for 24 h and immunostained for pp38 and phospho-FGFR (pFGFR). Scale bar, 10 μm. (**b**) Percentage of pFGFR$^+$ SCs out of total Sdc4$^+$ SCs (Mean ± s.e.m., $n = 3$ experiments, ≥20 myofibers scored/condition). (*c*) Percentage of phospho-p38$^+$ SCs of total Sdc4$^+$ SCs after 24 h treatment with DMSO or SU5402 (*$P < 0.05$ for Young DMSO vs. SU5402, two-way ANOVA. $n = 3$ experiments, ≥20 myofibers scored/condition). (**d–g**) Flow cytometric analysis of young and aged pp38$^+$ SCs with or without FGF-2 addition. Histograms of (**d**)

percent of Sdc4$^+$ events of total (max.) events and (**e**) p38αβ MAPK$^+$ events of Sdc4$^+$ subsets. Histograms of pp38$^+$ SCs (gated on Sdc4$^+$) following a 5 min FGF addition to (**f**) SCs in DMSO or (**g**) 25 μM SU5402 quantified (right) for FGF-2-induced increases in pp38$^+$ (n = 3 experiments. *P < 0.05, t test). (**h–i**) (**h**) CFDA-SE retention assay identifies self-renewed (Pax7$^+$/CFDA-SE$^+$), myofiber-associated SCs. (**i**) Average number of Pax7$^+$/CFDA-SE$^+$ SCs per myofiber length after a 72 h treatment with DMSO or SU5402 (*P < 0.05 for Young DMSO vs. SU5402; ***P< 0.001 for Young vs. Aged DMSO, two-way ANOVA). Mean ± s.e.m. for all.

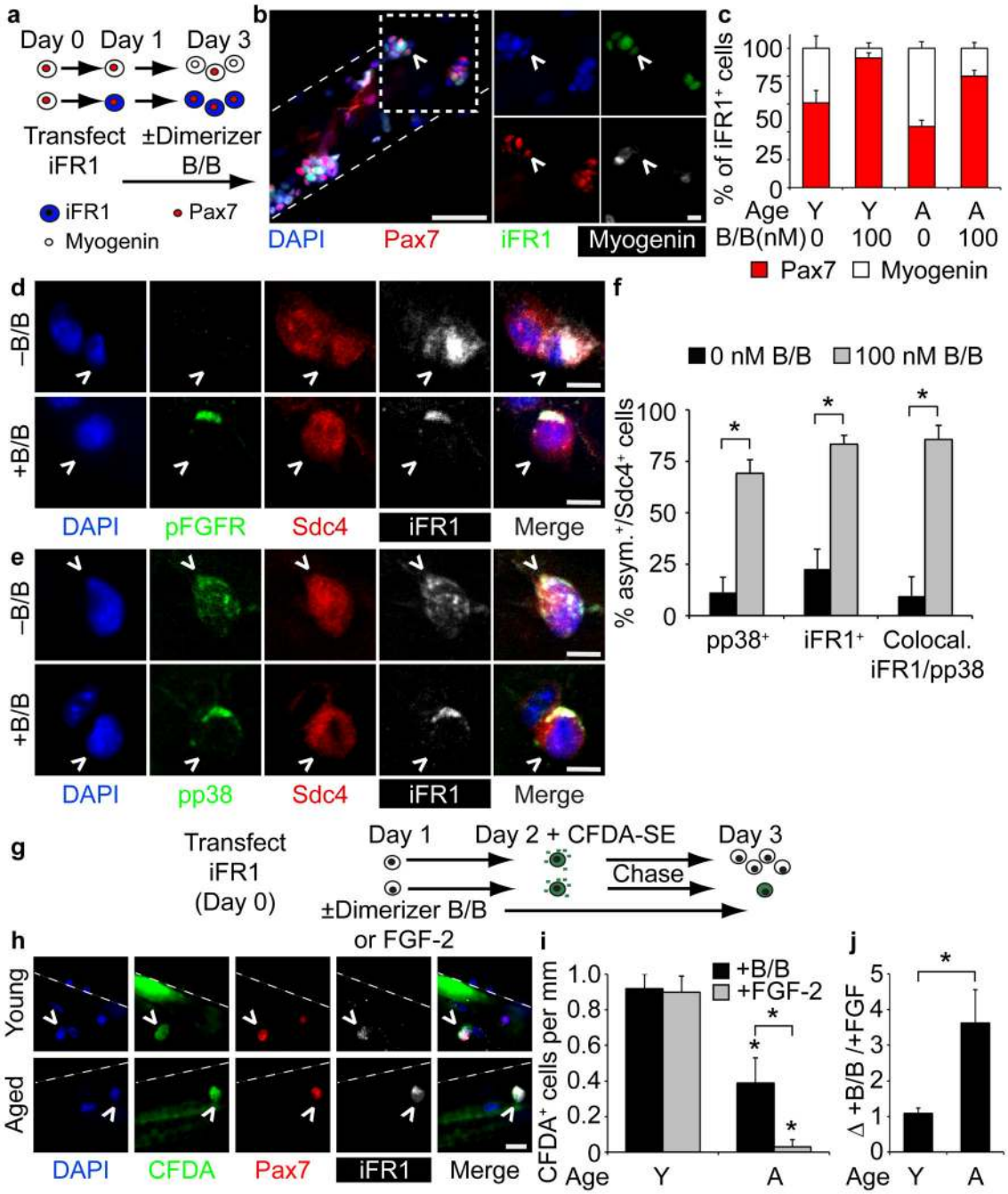

Figure 5. Constitutive FGFR1 signaling partially rescues self-renewal in aged SCs

(**a–c**) (**a**) Schematic for iFGFR1 (iFR1) transfection of young and aged SCs treated with or without Dimerizer B/B (B/B) to activate iFR1. (**b**) Image of iFR1$^+$ SCs (^ = HA-tagged-iFR1). Scale bars, 50 μm; inset (box), 10 μm. (**c**) Percentage of Pax7$^+$ or Myogenin$^+$ (of total iFR1$^+$ SCs) with or without Dimerizer B/B treatment ($P < 0.05$ for 0 vs.100 nM B/B (both Young and Aged), one-way ANOVA). (**d-f**) (**d**) Staining of pFGFR and (**e**) pp38 in young and aged iFR1$^+$ SCs (^), treated with or without Dimerizer B/B for 48 h. Scale bar, 5 μm. (**f**) The percentage of asymmetric pp38, asymmetric iFR1 or co-localized, asymmetric pp38 and

iFR1 Sdc4$^+$ SCs (*P < 0.05, t test. Mean ± s.e.m., n = 3 experiments, ≥30 myofibers). (**g-j**) (**g**) Schematic for CFDA-SE retention assay of iFR1 expressing SCs. (**h**) Label-retaining, iFR1-transfected young and aged SCs (^ = CFDA$^+$/Pax7$^+$/iFR1$^+$). Scale bar, 10 μm. (**i**) Average number of label-retaining SCs per myofiber length (*P < 0.05, for Young vs. Aged B/B treated, Young vs. Aged FGF-2 treated, Aged B/B treated vs. FGF-2 treated, two-way ANOVA) and (**j**) average fold-change for number of young and aged B/B treated label-retaining SCs vs. FGF-2 treated SCs (*P < 0.05, t test. Mean±s.e.m., n = 3 experiments, ≥20 myofibers).

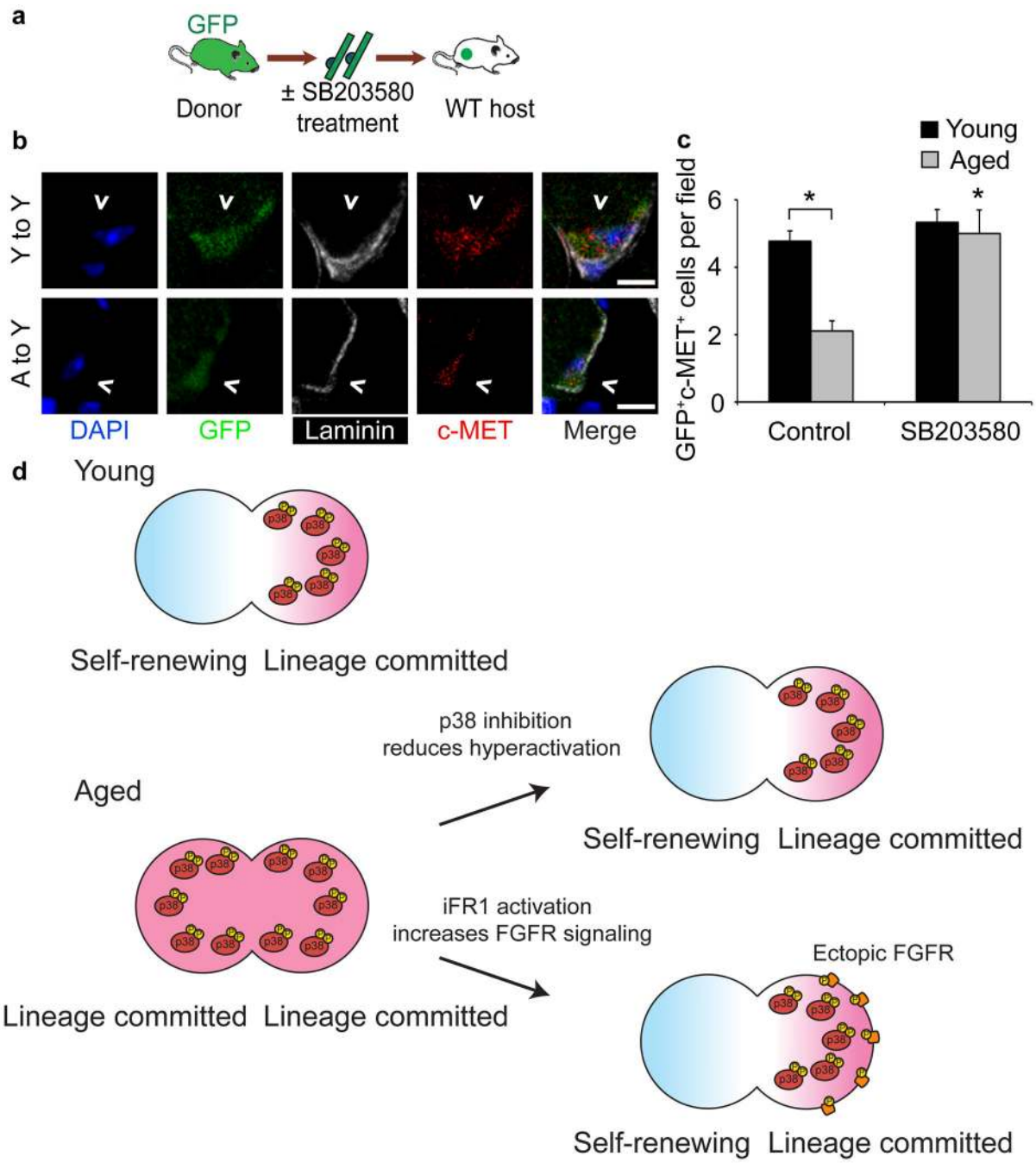

Figure 6. Partial p38αβ MAPK inhibition rescues aged SC engraftment

(**a–c**) (**a**) Schematic for heterochronic myofiber transplantation into young host muscles after overnight treatment with 10 μM SB203580 or FGF-2 (control). (**b**) Images of donor-derived SCs (^ = GFP$^+$/c-Met$^+$) in muscle sections 30 d post-transplantation. Scale bar, 5 μm. (**c**) Average number of donor-derived SCs per field (Mean ± s.e.m. $n = 3$ transplant recipients. *$P < 0.05$ for Aged Control vs.SB treated, Young vs. Aged Control, two-way ANOVA). (**d**) Model. Asymmetric p38αβ MAPK activation promotes self-renewal in young SCs generating a quiescent daughter and a lineage committed daughter cell. Elevated pp38

in aged cells prevents asymmetric p38αβ MAPK signal transduction generating two lineage committed daughter cells. Partial inhibition of p38αβ MAPK permits asymmetric p38αβ MAPK activation, restoring self-renewal in aged SCs. Ectopic activation of constitutively expressed iFR1 re-localizes iFR1 into an asymmetric signaling complex promoting asymmetric localization of active iFR1, resulting in asymmetric activation of p38αβ MAPK and self-renewal.